Chapter 8
Laser Micromachining

Jürgen Ihlemann

Abstract This chapter deals with the laser-based fabrication of surface structures by ablative material removal. Only microstructures with typical dimensions ranging from 100 to 1 mm are treated here. Only the use of pulsed lasers, mainly in the nanosecond pulse duration regime, is described, for fs-laser micromachining see Chap. 6. Only technical materials are treated, not biological material.

8.1 Basic Considerations

Laser micromachining of materials is used here in the sense that a laser beam is directed onto a solid material in a specific manner, so that controlled material removal takes place leading to a functional surface or 3D pattern. While the fundamentals of laser-material interactions are described in Chap. 3, we concentrate here more or less on a phenomenological description of the various irradiation concepts and the resulting surface structure or surface shape. As sufficient optical absorption is the main prerequisite of precise ablative laser processing, in most cases UV-lasers are applied. The short wavelength serves for high optical resolution at the same time.

8.2 Processing Limits

Micromachining by ablative removal of material is characterized by a threshold fluence F_{T}, i.e., the minimum energy per area that is required to start ablation, and the fluence dependent ablation rate $d(F)$, i.e., the ablation depth per laser pulse. If it is assumed that ablation takes place to that depth where the fluence has decreased

J. Ihlemann
Laser-Laboratorium Göttingen e.V., Hans-Adolf-Krebs-Weg 1, 37077 Göttingen, Germany
e-mail: juergen.ihlemann@llg-ev.de

to F_T due to absorption according to the Lambert Beer law, the ablation rate should behave like:

$$d(F) = \alpha^{-1} \log(F/F_T) \tag{8.1}$$

with the absorption coefficient α.

This behavior is approximately observed for strongly absorbing polymers like polyimide, but it does not hold for materials that change their absorption due to irradiation. This change can be a permanent increase because of chemical modification of the material or color center formation leading to the so called incubation behavior, or a transient change due to the formation of transient species with different absorption. In these cases often an effective absorption coefficient α_{eff} is defined, which is derived from the experimentally measured ablation curve $d_{exp}(F)$ according to:

$$\alpha_{eff} = d_{exp}^{-1} \log(F/F_T). \tag{8.2}$$

The structure resolution which can be reached by laser micromachining is limited on the one hand by the resolution of the light intensity profile on the surface (optical resolution) and on the other hand by the thermal distribution of the absorbed energy on the time scale of the pulse duration (thermal resolution). The optical resolution is given by:

$$A = \frac{\lambda}{2NA} \tag{8.3}$$

with the laser wavelength λ and the numerical aperture NA of the optical system used for the irradiation. Thus, the optical resolution can be improved by choosing a shorter wavelength and/or using a lens with larger numerical aperture. However, the numerical aperture influences the depth of focus DOF according to

$$DOF \sim \frac{\lambda}{NA^2}, \tag{8.4}$$

so that a higher NA leads to strongly increasing requirements concerning the ‘z-positioning’ of the surface to be machined. Therefore, the generation of small structures with high aspect ratio (ratio depth over lateral width) is rather difficult. For such deep holes, effects like *light channelling* have to be utilized.

The resolution limit given by thermal spreading of the absorbed energy is given by the heat diffusion length

$$L = 2(D\tau)^{1/2} \tag{8.5}$$

with the laser pulse duration τ and the thermal diffusivity D given by $D = \kappa\rho c_p$ (κ thermal conductivity, ρ density, c_p specific heat capacity of the irradiated material).

In Table 8.1 the excimer laser ablation rates (ablation depth per pulse) are listed for some often used materials. The data are given for pulse lengths of about 10–30 ns and laser spot diameters of the order of 100 µm. Actually, the ablation rate depends on these parameters, too. Especially at high fluences (5 J/cm^2 is already high in that sense), the ablation rate increases with growing pulse duration and with diminishing

Table 8.1 Ablation rates in nm/pulse of various materials at specific laser wavelengths at 5 J/cm^2

Material	157 nm	193 nm	248 nm	308 nm
Polyimide (PI)		200 [1]	650 [2]	1,150 [2]
Polymethylmethacrylate (PMMA)		500 [1]	4,000 [2]	
Polycarbonate (PC)			650 [3]	1,100 [3]
Polytetrafluoroethylen (PTFE)	600			
SF11-glass		140 [4]	170 [4]	
BK7-glass		170 [4]	600 [4]	
Fused silica	100 [5]	200 [6]	1,800 [6]	–
Al_2O_3-ceramic		30 [7]	100 [8]	230 [8]
MgO-ceramic			110 [8]	50 [8]
Copper			80 [9]	
Aluminium		800 [10]		
Molybdenum			30	

spot size [11, 12] due to the screening of the expanding product plume. Most of the lasers used for micromachining operate with ns-, ps-, or fs-pulses. There are two reasons for choosing ultrashort pulses: to increase the absorption by nonlinear effects and to reduce the heat affected zone (HAZ). Whereas a fs-pulse duration is required for efficient multiphoton absorption to treat transparent materials, for the reduction of unwanted heat effects like melt rims, the use of picosecond pulses seems to be sufficient. Ultrashort pulse processing is treated in a separate chapter. The wavelengths used for micromachining are in the range from vacuum ultraviolet (157 nm) to infrared (1,064 nm). CO_2-lasers with longer wavelengths (10.6 μm) are mainly used for macromachining, because the optical resolution does not allow shaping on the μm-scale. Beam delivery is accomplished either by direct spot writing or by mask projection.

8.3 Materials and Processes

8.3.1 Polymers

Organic polymers are well suited materials for UV-laser micromachining. Especially, polymers containing aromatic constituents (polyimide, polycarbonate, polyethersulfone, polyethylene-terephthalate (PET)) absorb very well in the near UV. Their threshold fluence is rather low; ablation can be easily performed at 248, 266, 308, or 351 nm wavelength. Polymers with linear chains without aromatic ring systems (polymethylmethacrylate (PMMA), polyethylene (PE)) have an absorption edge in the deeper UV, so that a wavelength of 193 nm is required for clean ablation. For fluorocarbon polymers like polytetrafluoroethylen (PTFE) even shorter wavelengths, e.g., 157 nm have to be applied (Fig. 8.1). Some new polymer materials have been specially developed for excellent 308-nm ablation performance (Fig. 8.1).

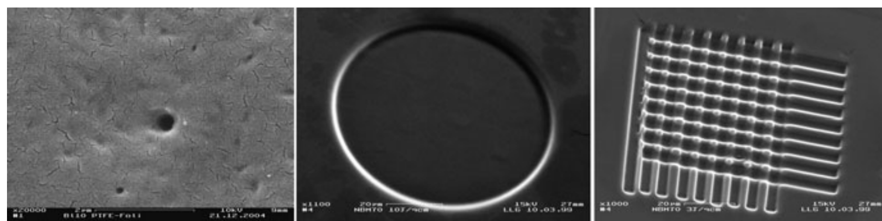

Fig. 8.1 Nanohole in PTFE ablated at 157 nm [13] (*left*) and ablation patterns in arylazophosphonate containing polymers designed for XeCl laser ablation [14] (*center, right*)

Photoablation of polymers has often been termed a 'cold' process, because in many cases very sharp contours with no evidence of heat effects are obtained. This does not mean that the ablated material remains cold, but because of the low thermal conductivity of the polymeric material and the efficient eduction of the absorbed energy with the ablation products, the heat effect on the remaining material is limited. Some weakly absorbing polymers exhibit a so called 'incubation behavior.' This means that the first few pulses do not lead to substantial ablation but to a material modification that leads to stronger absorption and substantial ablation for following pulses at the same site [15]. Even for fluences below the ablation threshold these changes may occurs. For instance, the transmission of a 40 μm thick PMMA film irradiated at 248 nm and a fluence of 40 mJ/cm^2 drops to 6% of its initial value after 1,000 pulses.

At high fluences the influence of the product plume on the ablation result becomes significant. The trailing part of a nanosecond pulse is already absorbed in the material cloud generated by the beginning part of the same pulse [2]. This leads to a saturation of the ablation rate with further increasing fluence. Furthermore, because of the 3D-expansion characteristics of the plume, the ablation rate depends on the lateral dimensions of the laser spot. A smaller spot will lead to a larger ablation rate at the same fluence. This means that even a completely homogeneous illumination of the mask in a mask projection set-up may lead to different ablated depths for different geometrical features. Similarly, changes of the pulse duration in the nanosecond regime lead to variations of the ablation depth. For instance, the ablation depth of polyimide at a laser wavelength of 248 nm and a fluence of 10 J/cm^2 amounts to 0.75 μm/pulse for a pulse duration of 20 ns, and 1.9 μm/pulse at 230 ns [2]. This can be explained by a more pronounced plume absorption in the case of shorter pulses, when the time is not sufficient for lateral dilution of the product plume.

The redeposition of ablated products (debris), which is very undesirable for most micro machining applications, can be diminished by choosing the adequate fluence. For the KrF-laser ablation of polyurethane for instance, at 100 mJ/cm^2 a lot of debris is deposited around the ablation holes. At 200 mJ/cm^2 the generated debris is greatly reduced, presumably because of the stronger fragmentation of the ablated polymer material into volatile, small molecular-weight compounds [16]. The distribution of surface debris can be further influenced by the ambient atmosphere. Lower pressure

leads to a wider, but more dilute distribution of the debris [17]. Similarly, ambient gases of low molecular weight (e.g., He) lead to a strong reduction of at least nearby debris.

The wall angle of laser generated holes or channels plays an important role for many micro machining applications. As a general rule, a higher fluence leads to a steeper wall. But in detail the wall angle can be tuned by choosing the effectively used numerical aperture of the optical system. This way even negative wall angles are possible [18]. Holes with very steep wall angles and consequently a high aspect ratio (depth over diameter) of 600 have been obtained by KrF-excimer laser ablation in various polymers like PMMA or polycarbonate [19].

8.3.2 Glass

Phenomenologically, glasses behave similar to organic polymers. Strongly absorbing glasses allow smooth ablation at low fluences, especially at 193 nm [20]. Lead glass can be machined also at 248 nm or even 308 nm [21]. CO_2-lasers can be used for polishing of lead glass [22]. But many glasses with low absorbance require high fluences to overcome the dielectric breakdown threshold. Often, in analogy to the incubation behavior of polymers, a two phase behavior with low ablation rate for the first pulses and increase of the ablation rate due to accumulation of absorbing defects is observed [6]. For highly transparent glass materials another interesting phenomenon has been observed. As the laser damage threshold at a surface is generally lower, when the beam propagates from a high refractive index material (glass) to a low refractive material (air) then the opposite way [23], a hole can be drilled from the backside into the material. There is practically no bulk absorption, ablation is initiated by rear surface absorption and continues because of the accumulation of surface defects at this rear surface. This behavior has been observed in the case of fused silica for UV-lasers [6] as well as for near-IR-lasers [24].

For extremely UV-transparent glasses like fused silica, irradiation at 193 nm leads to cracking, so that irradiation at 157 nm is required to obtain precisely machined structures (Fig. 8.2) [25]. The ablation rate can be precisely tuned between 10 and 100 nm per pulse by choosing a fluence between 1 and 10 J/cm^2, and a surface roughness of 5–15 nm rms can be achieved [5]. A 157 nm is also used to obtain smooth ablation of N-BK7 glass [26].

An important feature of glass processing is the remaining surface roughness at the bottom of ablated spots or channels. In case of ArF-laser processing of borocilicate glass (Pyrex) roughness values of $R_\mathrm{a} = 35 \ldots 150$ nm have been obtained, depending on fluence and irradiation procedure [28].

8.3.3 Ceramics

Many ceramic materials like alumina (Al_2O_3) or magnesia (MgO) have also weak UV-absorbance. Their sintered grain structure leads to light scattering and increased

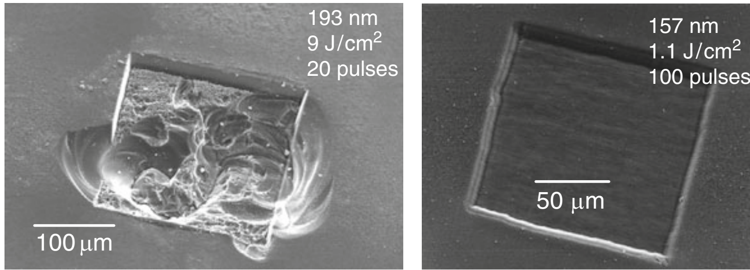

Fig. 8.2 Fused silica ablated at 193 nm and at 157 nm [27]

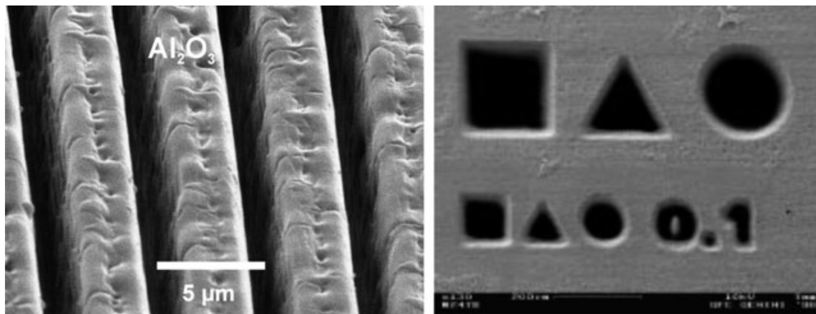

Fig. 8.3 Line pattern machined in alumina ceramic with an ArF-excimer laser [7] (*left*). Microgeometries in SiC structured with a frequency tripled YAG-laser at 355 nm [31] (*right*)

defect density compared to single crystals. High fluences ($> 1\,J/cm^2$ at 248 nm) are necessary to obtain ablation. A plasma mediated process is observed leading to smoothing of the surface (Fig. 8.3). This plasma mediated process has been observed also for single crystal MgO [29]. Stronger absorbing nitride materials (Si_3N_4) exhibit a somewhat lower ablation threshold ($< 1\,J/cm^2$ at 248 nm), but precise patterning is possible only at high fluences, too [30]. Precise ablation of SiC and Si_3N_4 is possible also with YAG-lasers, either at the fundamental wavelength or at the second or third harmonic [31] (Fig. 8.3). The roughness of side walls in the case of IR-laser (CO_2 and YAG) processing is significantly larger than that for excimer laser processing [32].

8.3.4 Metals

Metals exhibit high reflectivities and low penetration depths. UV-lasers are applied, because the reflectivity decreases in the UV. The penetration depth is still limited to a few 10 nm; but because of heat conduction the absorbed energy is transferred into deeper regions and the ablation rate can significantly exceed the optical absorption length. On the other hand, the high thermal conductivity leads to noticeable melt effects (Fig. 8.4) like burrs around ablated areas [33]. These observations suggest

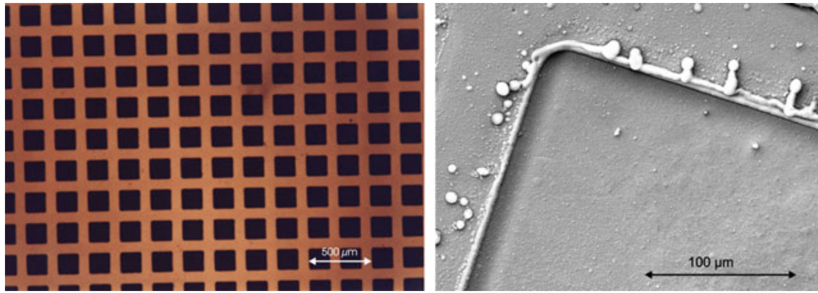

Fig. 8.4 Copper grid on fused silica made by laser micromachining, thickness of the copper layer: 500 nm; laser parameters: 193 nm, 450 mJ/cm^2, 5 pulses. (*Left*: optical microscopy, *right*: scanning electron microscopy)

strong hydrodynamic contributions to the ablation process of metals even in the UV (248 nm) [9]. The importance of the absorption and heating of the plasma plume has been pointed out [34, 35].

8.3.5 Layer Ablation

In addition to bulk micro machining, laser ablation can be used for the patterning of thin films. If the threshold fluence of the film material is significantly lower than that of the substrate material, it is easy to remove the film without damaging the substrate. This is the case for polymer films on metal or glass substrates. The substrate acts as stop layer and the process can be controlled easily, as some excessive pulses do not alter the result. On the other hand, the removal of a metal film from a polymer substrate requires more controlled conditions to avoid substrate damage [36]. In addition, it has to be taken into account, that the ablation threshold of metal films depends on the film thickness, if nanosecond laser pulses are applied [37]. This is caused by the high thermal conductivity of the metal, which serves for a rapid thermal spreading of the absorbed energy over the whole film thickness, so that thicker films get less heated compared to thinner films at the same laser fluence. The achievable resolution is limited by *edge curling* effects [38].

If the substrate is transparent at the laser wavelength, in addition to the standard *front side ablation* also a *rear side ablation* configuration is possible [39]. This means that the laser beam is absorbed in the film after passing through the transparent substrate. Fused silica substrates are sufficiently transparent to enable rear side ablation with wavelengths in the whole UV and visible range above 190 nm. For near UV and visible lasers, even other glass substrates can be applied (BK7); rear side ablation using a 157 nm-laser has been demonstrated with CaF_2-substrates [40]. If the layer system to be patterned is transparent at the laser wavelength, an underlying absorber layer can be applied, which enables rear side ablation, but does not obstruct the functionality [e.g., of a mirror layer system used in a front side application (Fig. 8.5)].

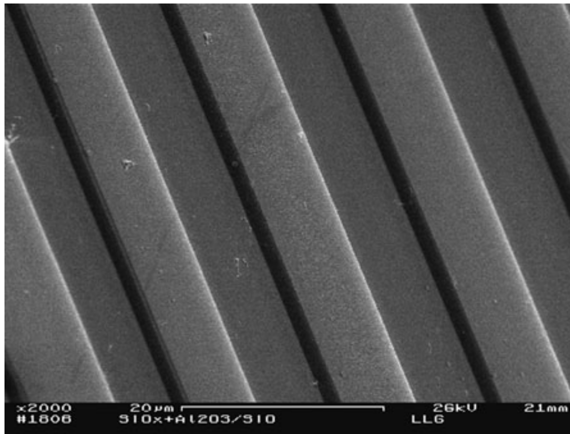

Fig. 8.5 Single pulse rear side ablation of a Al_2O_3/SiO_2-multilayer dielectric coating with underlying SiO-absorber layer on fused silica, ArF-excimer laser, 500 mJ/cm^2 [41]

8.3.6 Indirect Ablation

There are several methods of laser machining, where the laser radiation is not directly coupled into the material to be ablated, but by means of an auxiliary absorber material. This is particularly of interest, if the material is transparent at the ablation wavelength. Then the laser light can be delivered to the absorber (instead of directly to the workpiece to be machined), leading to various kinds of indirect ablation:

In the case of "laser induced backside wet etching" (LIBWE) [42] the backside of the sample to be machined is in contact with an absorbing liquid, which may be an alcoholic or aqueous solution of a dye absorbing at the laser wavelength. The energy is coupled into the rear surface of the workpiece by heating this absorber liquid. This method was successfully applied to pattern fused silica, crystalline quartz [43], and sapphire [44]. The etch rate is rather low compared to direct ablation, but this enables the precise depth profiling. Structure resolution down to 1 micron has been achieved. The main advantage of this method is, that the laser wavelength does not have to be adapted to the material to be machined, but only to the absorbing dye, so that the rather convenient wavelength 308 nm can be used for glass machining.

Another method is based on non permanent, but laser induced indirect absorption. In this process called 'laser-induced plasma-assisted ablation' (LIPAA) [45], a metallic sample is positioned behind the transparent workpiece (e.g., fused silica). The laser pulse causes a plasma plume expanding from the metal to the backside of the workpiece, which is then able to absorb light via the deposited metallic layer.

Especially for the micro machining of fused silica a variety of methods has been developed to overcome the problem of insufficient absorption. An overview on direct and indirect methods is shown in Table 8.2.

Table 8.2 Direct and indirect ablation methods for micromachining of fused silica

Method	Type	Mode of operation	References
DUV (193 nm)	Direct	(Surface-) Defect absorption	Ihlemann et al. [6]
VUV (157 nm)	Direct	Near bandgap absorption	Herman et al. [5]
Soft x-ray (10 nm)	Direct	Laser plasma soft x-rays	Makimura et al. [46]
Multiwavelength	Direct	VUV → transient absorption UV → ablation	Sugioka et al. [47]
Femtosecond	Direct	Multiphoton absorption	Varel et al. [48] Krüger et al. [49]
LIBWE	Indirect	Laser induced backside wet etching	Wang, Niino, Yabe [42]
LIPAA	Indirect	Laser induced plasma assisted ablation	Zhang, Sugioka et al. [45]
LESAL	Indirect	Laser etching at a Surface Adsorbed Layer	Zimmer et al. [50]
LIBDE	Indirect	Laser induced backside dry etching	Hopp et al. [51]

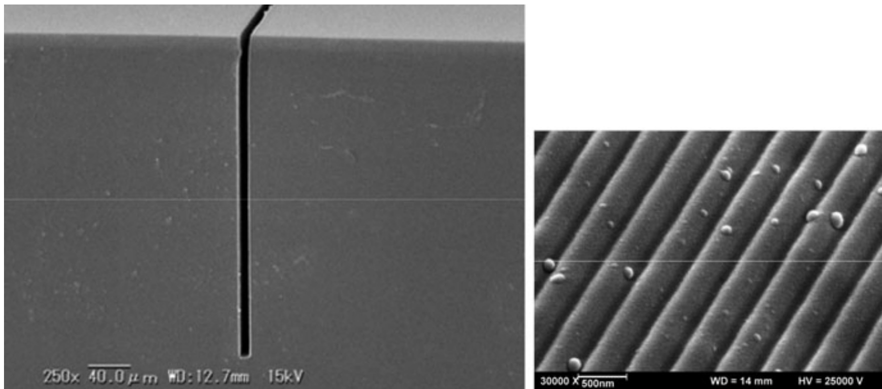

Fig. 8.6 Deep trench in silica glass fabricated by the LIBWE method; laser: 248 nm, 1 J/cm^2, 20,000 pulses (*left*) [53]. 400 nm-line pattern in fused silica made by solid-coating-absorption-mediated ablation; laser: 193 nm, 16 J/cm^2, 1 pulse (*right*) [52]

The absorbing medium for indirect ablation does not have to be a liquid. Good results have also been obtained by using adsorbed layers [50] or, for single pulse machining, metal [51] or dielectric [52] absorber layers. Whereas LIBWE seems to the optimum choice for generating deep trenches with high aspect ratio [53] (Fig. 8.6), LIBDE is more appropriate to obtain either high resolution or a large single pulse ablation rate [52, 54].

8.4 Hole Drilling

The straightforward application of laser ablation in micromachining is hole drilling. In the simplest form it is accomplished by focusing a laser beam onto the work-piece and applying as many pulses as required to obtain a via hole (through hole) or a pocket hole (blind hole). With this method a reasonable quality of the holes is obtained only, if a Gaussian laser beam is used, e.g., in the case of solid state lasers (YAG). In the case of flat top beam profiles (excimer laser), perfect quality can be achieved by mask imaging. Depending on laser energy, size of the hole and material, one hole at a time is made with a pinhole mask, or parallel processing of a multihole pattern is performed using a complex multihole mask. For comparatively large hole diameters, alternatively to this percussion mode (laser spot is fixed with regard to the work piece), the trepanning mode can be applied, where the laser spot is guided on a circle, so that a disc is cut out of the work piece. This is already the route to laser cutting, which is more or less a macromachining process and is not treated here.

An important application of micro hole drilling is the fabrication of nozzle plates for ink jet printers. In a standard process, several rows of holes are drilled simultaneously using an excimer laser and a mask projection system. These holes in polyimide have diameters of about 10–50 μm. In such configurations, it has to be taken into account, that even in the case of homogeneous illumination, nonuniform hole depths are obtained due to geometrical effects of the plume shielding [55]. Depending on the required geometries, materials and hole dimensions, holes in multilayer printed circuit boards are made by excimer laser drilling [56], or for instance in a combined process, where copper layers are drilled with a frequency tripled YAG-laser and the intermediate dielectric layers are removed by a CO_2-laser [57]. Using CO_2-lasers, hole dimensions down to 10 μm are possible in polyimide and glass material [58].

Also in semiconductor device fabrication and production of photovoltaic devices there are several applications of hole drilling. One example is the drilling of silicon carbide wafers [59]. Using a frequency tripled diode pumped solid state laser at 355 nm, through and blind holes of 60 μm diameter with aspect ratios of 5–6 have been obtained (Fig. 8.7). For the back contacting of solar cells, processes with parallel drilling of up to 5,000 holes using 1,047 nm-laser radiation have been developed [60].

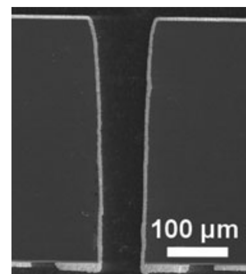

Fig. 8.7 355 nm-laser drilled hole in SiC after etching and metallization [59]

Fuel injection nozzles in steel for gasoline or Diesel engines with typical diameters of around 100 μm are made mainly by diode pumped YAG-lasers, either with the fundamental wavelength or using the second or third harmonic [61,62]. Not only size reduction but also specifically shaped holes (tapers) are of interest.

Other applications of laser hole drilling are in the biomedical field. One example is the fabrication of nozzles for the so called pulmonary drug delivery. These nozzles often have to be strongly conical with an exit diameter of about 1 μm. Excimer lasers are used to fabricate such disposable nozzle plates [63].

8.5 Patterning of Thin Films

Applications of thin film patterning include the fabrication of thin film photovoltaic cells (CIS, amorphous silicon) and flat panel displays (ITO patterning) [64]. Excimer laser patterning of Cr films on glass substrates has been investigated [65] and applied to the fabrication of Cr-masks [66, 67].

One micron thick TiN coatings on steel have been patterned using a Nd:YAP laser at 1,078 nm and at its second and third harmonic [68]. Microcraters with diameters of 3–5 micron and 1 micron depth have been obtained at all three wavelengths. By generating such microcrater arrays, the durability of lubricated sliding could be increased by 25% compared to that of the original TiN film.

By micropatterning diamond films with Nd:YAP (1,078 nm) and KrF-excimer lasers, IR-antireflection coatings could be machined [69]. The patterns consist of hole arrays or grooves with 3 micron period.

8.5.1 Dielectric Masks

A number of studies have been performed to investigate the microfabrication of masks and diffractive phase elements by laser patterning of dielectric layers. A typical application for the patterning of multilayers for optical applications is the fabrication of dielectric optical masks. Dielectric masks can be applied for high-intensity laser applications, where metal masks (Cr on quartz) would be easily damaged [70]. Multilayer stacks of alternating high refractive index and low refractive index (HfO_2/SiO_2) can be ablated by an ArF-excimer laser, because HfO_2 is absorbing at 193 nm. Although the thickness of the film is more than 1 μm, under certain conditions sub-μm edge definition is achieved in the case of rear side ablation [71].

If both materials of the dielectric layer stack are transparent at 193 nm, the ablation of these systems has to be performed either at even shorter wavelengths (Vacuum-UV) [72] or with an absorbing subsidiary layer. Thus, dielectric mirrors with high reflectivity at 193 nm consisting of a stack of alternating SiO_2- and Al_2O_3-layers were patterned by depositing a 193 nm-absorbing HfO_2- or SiO-layer

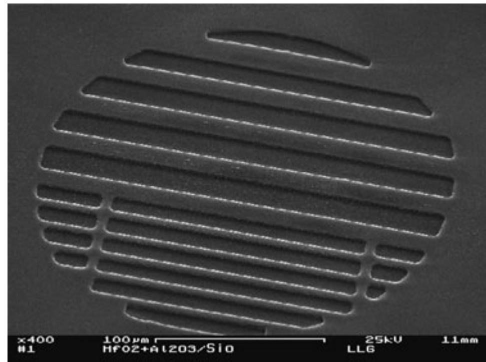

Fig. 8.8 Dielectric mask fabricated by single pulse rear side ablation of a Al_2O_3/SiO_2-multilayer dielectric coating with underlying HfO_2-absorber layer on fused silica, ArF-excimer laser, 1.3 J/cm^2 [73]

between substrate and HR-stack and ablating in a rear side configuration [73] (Fig. 8.8). It is even possible to fabricate grey level masks by ablating only a defined number of single layers instead of the whole stack [74]. As this process works only by front side ablation, the edge definition of the ablated structures is limited.

8.5.2 Diffractive Optical Elements

Laser film patterning is the ideal method for the flexible generation of diffractive optical elements (DOE). Specifically, diffractive phase elements (DPE) enable the generation of complex irradiation patterns without substantial optical system energy losses. In many cases a computer generated two-dimensional phase function is transferred into an optically effective phase controlling element by fabricating a surface relief on a transparent substrate.

Diffractive optical elements can be characterized as amplitude or phase elements. The simplest phase element to be used at a wavelength λ is a binary surface relief structure on a material of refractive index n with a depth modulation of $d = \frac{\lambda}{2(n-1)}$. Lateral structure dimensions are of the order of a few microns depending on the optical configuration and the coherence parameters of the light for which the DOE is designed. For a DOE made of a polymer material, to be used in the visible spectral range, surface structures with a depth of about 0.5 micron and lateral dimensions of 5 micron are required. These dimensions are easily accessible by excimer laser ablation. Some attempts have been made to fabricate DOEs by laser ablation, either on the basis of pixel by pixel irradiation [75,76] or image based using chrome masks [77]. Multilevel DOEs could be produced in polymers by excimer laser ablation using a half tone mask [78]. DOEs that can be used for UV laser applications require the processing of fused silica or other materials with high UV transmission. Such DOEs have been fabricated on the basis of dielectric mask projection [79].

For the fabrication of diffractive phase elements from SiO_2 without the need of direct ablation of fused silica the following three-step-method has been suggested [81]: (1) A UV-absorbing coating of silicon monoxide (SiO) is deposited on a fused

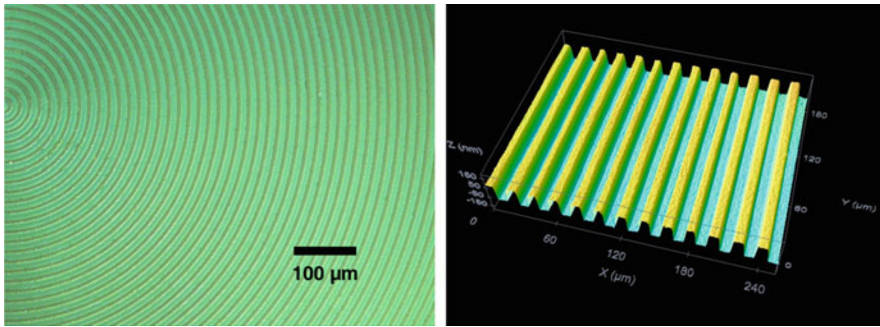

Fig. 8.9 Diffractive phase elements made by rear side ablation of SiO layers and subsequent oxidation [80]

silica substrate. (2) The SiO-coating is patterned by excimer laser ablation to form the desired phase structure. (3) The SiO-material is oxidized to UV-transparent silicon dioxide (SiO_2). Phase elements fabricated with this method are shown in Fig. 8.9.

8.6 Fabrication of Micro Optics and Micro Fluidics

One large field of laser micro machining is that of generating micro optical structures. This is understandable, because the precision or resolution required here matches roughly the ultimate precision or resolution which is possible with standard light-based manufacturing processes, both given by the wavelength scaled with a factor of the order of 1. This led to a variety of processes for fabricating optical components like micro lenses, gratings, or complex diffractive structures.

8.6.1 Gratings

Laser micromachining of optical grating structures has been a subject of study for a long time. This work aimed either at the demonstration of high resolution capability of the ablation process or at the fabrication of real gratings to be used, e.g., as coupling gratings for planar waveguides. The spatially periodic intensity pattern needed for the generation of a (one dimensional) periodic surface structure with a periodicity of the order of the wavelength of light can be understood generally as the consequence of the interference of two beams. Several optical arrangements are possible: The interfering beams may be generated by a partially reflecting beam splitter or by a diffractive beam splitter and recombined either by using beam superposition in a Talbot interferometer [82, 83] or by imaging methods, using, e.g., a Schwarzschild type objective [27]. Depending on a specific configuration, the coherence properties of the applied laser radiation may be crucial for the development of

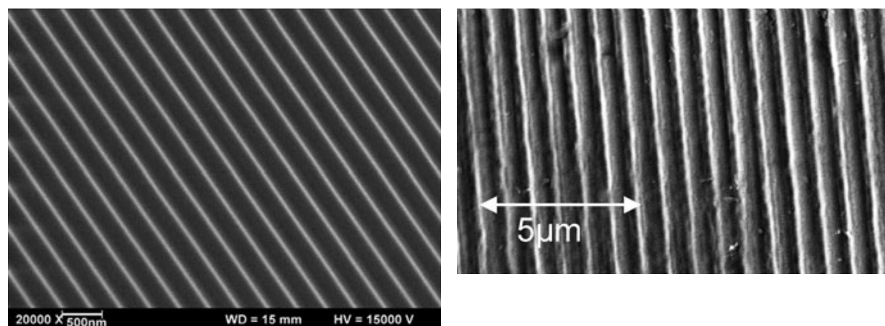

Fig. 8.10 331 nm-period grating in polyethersulfone fabricated using a KrF-laser in combination with a two grating interferometer [84] (*left*). 800 nm-period-grating in fused silica made by F_2-laser ablation [66] (*right*)

the periodic patterns. An arrangement of two gratings, where the second grating recombines the ± first diffraction orders generated at the first grating, allows for efficient submicron patterning with high contrast even with only partially coherent laser light [84].

Such grating designs are used in several micro-optic applications such as grating demultiplexers for telecommunication components, light couplers for planar optical waveguides, Bragg reflectors, and alignment grooves for liquid crystals [85, 86]. Submicron periodic structures, which are required for ultraviolet, visible, and near-infrared spectral applications, have been structured by UV-laser ablation with nanosecond (ns) duration pulses on polymer [87–90] and borosilicate glass [91] surfaces. For the fabrication of gratings on metals or crystalline optical materials femtosecond excimer lasers, for the treatment of weakly absorbing materials like fused silica [66] or metal oxide waveguides [92], F_2-lasers have been applied (Fig. 8.10).

8.6.2 *Micro Lenses*

It is very attractive to fabricate micro lenses by laser ablation, because, if the basic problems of creating a smooth, three dimensional surface in an optical material are solved, a great variety of lens shapes should be possible (aspheric etc.). The processing of cylindrical lenses is rather straightforward, if a flexible mask technology is applied [7] (Fig. 8.11). In the case of processing glass, the ablation debris is one of the major problems, which can be solved by ablating in a vacuum or by applying additional cleaning procedures. For the generation of spherical lenses, an approach based on scanning a polymer surface with an excimer beam along well-chosen multiple concentric contours was applied [93, 94]. This way microlenses of arbitrary shape can be realized. Lens arrays could be fabricated by the so

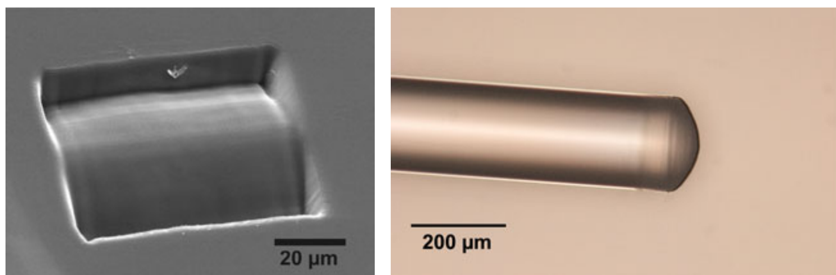

Fig. 8.11 Cylindrical microlens fabricated in BK7-glass at 193 nm with a variable mask technique [7] (*left*). Lens machined at a fused silica fiber tip by 157-nm-ablation [99] (*right*)

called synchronized-image-scanning (SIS) in combination with half tone masks [95]. Besides the fabrication of refractive lenses, also the machining of diffractive (Fresnel-type) lenses in polymers [96] and glasses [97] has been demonstrated.

There have been made some attempts to integrate microlenses in optical fiber tips by laser machining. Using a CO_2-laser the processing is more or less based on a defined melting process [98]. For precise shaping of fused silica fibers, a VUV-laser emitting at 157 nm has to be applied. Two different techniques for the fabrication of microlenses directly on the end face of multimode silica fibers have been demonstrated using a F_2-laser processing station [99]. The first method is based on a mask projection arrangement perpendicular to the fiber axis. The fiber is rotated axially while the laser cuts through the fiber, yielding a spherically shaped tip with radius defined by the mask dimensions (Fig. 8.11). For the second technique, a uniform ablation spot is projected onto the fiber end face in axial direction and steered along a trajectory of overlapping concentric circles. The lens profile is controlled by the spot size, the number of circles in the trajectory, and the scanning speed. Strong 157 nm absorption by the silica glass facilitates precise structuring without microcrack formation in both cases. The surface quality of the fiber-lenses is characterized by $\sim$40 nm rms roughness with good control of the surface profile. Optical beam profiling indicates the possibility for creating spot sizes of $1/5$ the core diameter at the fiber output. Good results have been obtained also for processing single mode fibers [100].

8.6.3 Micro Fluidics

To machine microfluidic devices, several aspects of channel fabrication and surface texturing have been investigated. Using ArF-excimer lasers, channels or channel systems with typical dimensions of 10–50 µm in depth and width were made in polymers [101, 102] and borosilicate glass [103] (Fig. 8.12). Even in fused silica microchannels could be fabricated using a laser wavelength of 193 nm [7]. Though with a Nd:YAG laser at 355 nm smooth channels in glass without cracks could be

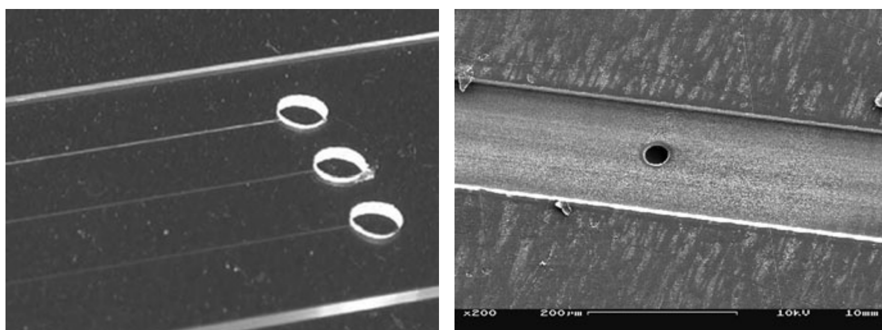

Fig. 8.12 Microchannel systems machined in glass with an ArF-laser (*left*) and in Teflon using a F_2-laser [13] (*right*)

obtained under well controlled conditions [104], and even at 532 nm the cutting of borosilicate glasses is possible [105], for the fabrication of precise grooves in weakly absorbing glasses the use of a F_2-laser seems to be more appropriate [106]. Microfeatures produced in N-BK7-glass using a F_2-laser have been replicated by polydimethylsiloxane (PDMS) moulding [107]. The obtained stamps have been used then to print arrays of fluorescent molecules with submicron fidelity. Hole arrays ablated in BK7 have been used to fabricate microneedle arrays by micromolding [20]. Such needle arrays are used in biomedical applications like gene and drug delivery.

To obtain microchannels in quartz glass with a nanosecond 1,064-nm-YAG-laser, very high laser fluences (up to 600 J/cm^2) have been applied to perform laser induced plasma processing [108].

8.7 Conclusions

Micromachining by laser ablation is a versatile tool for the generation of surface patterns and three-dimensional structures. Processing of any kind of technical materials like polymers, glass, ceramics, and metals is possible. Laser wavelength and pulse duration have to be adapted to the specific material and processing task. For precise machining of transparent materials the use of deep UV or vacuum UV wavelengths is ideal; for high-resolution patterning of metals ultrashort pulse lasers (ps or fs) are suitable. Thin films are preferably patterned by mask projection using flat top beams of excimer lasers. For the processing of transparent materials like fused silica a number of indirect ablation methods have been established, where the laser is absorbed by an auxiliary material, which is in contact with the sample surface. Laser ablation can be utilized for hole drilling and the machining of microfluidic devices like nozzles and channel systems. In addition, the fabrication of micro-optics like gratings, phase masks, micro lenses, and diffractive optical elements has been demonstrated.

References

1. V. Srinivasan, M.A. Smrtic, S.V. Babu, J. Appl. Phys. **59**(11), 3861 (1986)
2. H. Schmidt, J. Ihlemann, B. Wolff-Rottke, K. Luther, J. Troe, J. Appl. Phys. **83**(10), 5458 (1998)
3. H. Schmidt, Physikalisch-chemische Aspekte des excimerlaserinduzierten Ablationsprozesses an Polymeren. Phd, Göttingen (1994)
4. B. Wolff-Rottke, H. Schmidt, J. Ihlemann, in Laser treatment of materials (ECLAT'92), ed. by B.L. Mordike (DGM Informationsgesellschaft, 1992), pp. 615–620
5. P.R. Herman, R.S. Marjoribanks, A. Oettl, K. Chen, I. Konovalov, S. Ness, Appl. Surf. Sci. **154**, 577 (2000)
6. J. Ihlemann, B. Wolff-Rottke, P. Simon, Appl. Phys. A Mater. Sci. Process. **54**(4), 363 (1992)
7. J. Ihlemann, B. Wolff-Rottke, Appl. Surf. Sci. **106**, 282 (1996)
8. J. Ihlemann, A. Scholl, H. Schmidt, B. Wolff-Rottke, Appl. Phys. A Mater. Sci. Process. **60**(4), 411 (1995)
9. J. Arnold, F. Dausinger, in ECLAT (1990), p. 859
10. I. Horn, M. Guillong, D. Gunther, Appl. Surf. Sci. **182**(1–2), 91 (2001)
11. M. Eyett, D. Bäuerle, Appl. Phys. Lett. **51**(24), 2054 (1987)
12. B. Wolff-Rottke, J. Ihlemann, H. Schmidt, A. Scholl, Appl. Phys. A Mater. Sci. Process. **60**(1), 13 (1995)
13. M. Rauh, UV-Laser-Mikrostrukturierung von Polytetrafluorethylen für biophysikalische Anwendungen. Master, Göttingen (2005)
14. M.N. Nobis, C. Scherer, O. Nuyken, F. Beinhorn, J. Ihlemann, Macromol. Mater. Eng. **275**(2), 1 (2000)
15. S. Küper, M. Stuke, Appl. Phys. A Mater. Sci. Process. **49**(2), 211 (1989)
16. S. Küper, J. Brannon, K. Brannon, Appl. Phys. A Mater. Sci. Process. **56**(1), 43 (1993)
17. S. Küper, M. Stuke, Appl. Phys. Lett. **60**, 1633 (1992)
18. B. Burghardt, H.J. Kahlert, D. Basting, in Laser Treatment of Materials, ed. by B. Mordike (Oberursel, 1992), p. 609
19. S. Lazare, J. Lopez, F. Weisbuch, Appl. Phys. A Mater. Sci. Process. **69**, 1 (1999)
20. A.A. Tseng, Y.T. Chen, C.L. Chao, K.J. Ma, T.P. Chen, Optics and Lasers in Eng. **45**(10), 975 (2007)
21. C. Buerhop, N. Lutz, R. Weissmann, M. Geiger, in Laser Treatment of Materials (DGM Informationsgesellschaft, Oberursel, 1992), pp. 603–608
22. C. Buerhop, B. Blumenthal, R. Weissmann, N. Lutz, S. Biermann, Appl. Surf. Sci. **46**(1–4), 430 (1990)
23. M.D. Crisp, N.L. Boling, G. Dube, Appl. Phys. Lett. **21**, 364 (1972)
24. A. Salleo, T. Sands, F.Y. Genin, Appl. Phys. A Mater. Sci. Process. **71**(6), 601 (2000)
25. A.A. Tseng, physica status solidi (a) **204**(3) (2007)
26. P.E. Dyer, C.D. Walton, Appl. Phys. A Mater. Sci. Process. **79**(4), 721 (2004)
27. J. Ihlemann, M. Schulz-Ruhtenberg, T. Fricke-Begemann, in Eighth International Conference on Laser Ablation, vol. 59 (Institute of Physics Publishing, 2007), pp. 206–209
28. B. Keiper, T. Petsch, H. Exner, Excimer Laser Technology (Springer, Berlin, 2005), chap. Micro-Processing of Borosilicate Glass and Polymers, pp. 201–219
29. L. Dirnberger, P.E. Dyer, S. Farrar, P.H. Key, P. Monk, Appl. Surf. Sci. **69**(1–4), 216 (1993)
30. J. Heitz, J.D. Pedarnig, D. Bäuerle, G. Petzow, Appl. Phys. A Mater. Sci. Process. **65**(3), 259 (1997)
31. R. Weichenhain, A. Horn, E.W. Kreutz, Appl. Phys. A Mater. Sci. Process. **69**, 855 (1999)
32. I. Miyamoto, H. Maruo, in Proc. SPIE, vol. 1279 (1990), p. 66
33. D. Breitling, A. Ruf, F. Dausinger, in Proc. SPIE, vol. 5339 (2004), pp. 49–61
34. J.G. Lunney, R. Jordan, Appl. Surf. Sci. **127**, 941 (1998)
35. R. Jordan, J.G. Lunney, Appl. Surf. Sci. **127**, 968 (1998)
36. P.E. Dyer, D.M. Karnakis, P.H. Key, D. Sands, Appl. Surf. Sci. **109**, 168 (1997)

37. E. Matthias, M. Reichling, J. Siegel, O.W. Käding, S. Petzoldt, H. Skurk, P. Bizenberger, E. Neske, Appl. Phys. A Mater. Sci. Process. **58**(2), 129 (1994)
38. J.E. Andrew, P.E. Dyer, R.D. Greenough, P.H. Key, Appl. Phys. Lett. **43**, 1076 (1983)
39. J. Ihlemann, B. Wolff-Rottke, Appl. Surf. Sci. **86**(1–4), 228 (1995)
40. D. Schäfer, J. Ihlemann, G. Marowsky, P.R. Herman, Appl. Phys. A Mater. Sci. Process. **72**(3), 377 (2001)
41. J. Ihlemann, J. Békési, J.-H. Klein-Wiele, P. Simon, Laser Chemistry 2008 (2008), Article Id. 623872.
42. J. Wang, H. Niino, A. Yabe, Appl. Phys. A Mater. Sci. Process. **68**(1), 111 (1999)
43. J. Wang, H. Niino, A. Yabe, Appl. Phys. A Mater. Sci. Process. **69**, 271 (1999)
44. X.M. Ding, T. Sato, Y. Kawaguchi, H. Niino, Jap. J. Appl. Phys. Part 2-Lett. **42**(2B), L176 (2003)
45. J. Zhang, K. Sugioka, K. Midorikawa, Opt. Lett. **23**(18), 1486 (1998)
46. T. Makimura, H. Miyamoto, Y. Kenmotsu, K. Murakami, H. Niino, Appl. Phys. Lett. **86**, 103111 (2005)
47. K. Sugioka, S. Wada, Y. Ohnuma, A. Nakamura, H. Tashiro, K. Toyoda, Appl. Surf. Sci. **96**, 347 (1996)
48. H. Varel, D. Ashkenasi, A. Rosenfeld, M. Wähmer, E.E.B. Campbell, Appl. Phys. A Mater. Sci. Process. **65**(4–5), 367 (1997)
49. J. Krüger, W. Kautek, Appl. Surf. Sci. **96**, 430 (1996)
50. K. Zimmer, R. Böhme, B. Rauschenbach, Appl. Phys. A Mater. Sci. Process. **79**(8), 1883 (2004)
51. B. Hopp, C. Vass, T. Smausz, Appl. Surf. Sci. **253**(19), 7922 (2007)
52. J. Ihlemann, Appl. Phys. A Mater. Sci. Process. **93**(1), 65 (2008)
53. Y. Kawaguchi, H. Niino, T. Sato, A. Narazaki, R. Kurosaki, in Eighth International Conference on Laser Ablation, vol. 59 (Institute of Physics Publishing, 2007), pp. 380–383
54. B. Hopp, C. Vass, T. Smausz, Z. Bor, J. Phys. D: Appl. Phys. **39**(22), 4843 (2006)
55. B. Burghardt, S. Scheede, R. Senczuk, H.J. Kahlert, Appl. Phys. A Mater. Sci. Process. **69**(7), 137 (1999)
56. F.G. Bachmann, Appl. Surf. Sci **46**, 254 (1990)
57. M. Heßling, J. Ihlemann, S. Puschmann, G. Marowsky, M. Loff, M. Novotny, B. Radinger-Dombert, Laser-Praxis **3**, 14 (2001)
58. P.E. Dyer, I. Waldeck, G.C. Roberts, J. Phys. D: Appl. Phys. **30**, 19 (1997)
59. O. Krüger, G. Schöne, T. Wernicke, W. John, J. Würfl, G. Tränkle, in Eighth International Conference on Laser Ablation, vol. 59 (Institute of Physics Publishing, 2007), pp. 740–744
60. A. Schoonderbeek, R. Kling, A. Ostendorf, R. Grischke, R. Meyer, R. Brendel, in Proc. ALAC (2007)
61. J. Clarke, J. Profeta, in Advanced Laser Applications Conference & Exposition, ed. by D. Roessler, N. Uddin, B. Tang (Ann Arbor, 2004), p. 94
62. L. Herbst, J.P. Quitter, G.M. Ray, T. Kuntze, A.O. Wiessner, S.V. Govorkov, M. Heglin, in Proc. SPIE, vol. 4968 (2003), p. 134
63. T. Lizotte, Industrial Laser Solutions **17** (2002)
64. J. Chae, S. Appasamy, K. Jain, Appl. Phys. Lett. **90**, 261102 (2007)
65. S.K. Lee, S.J. Na, Appl. Phys. A Mater. Sci. Process. **68**(4), 417 (1999)
66. J. Ihlemann, S. Müller, S. Puschmann, D. Schäfer, M. Wei, J. Li, P.R. Herman, Appl. Phys. A Mater. Sci. Process. **76**(5), 751 (2003)
67. A. Yick, J. Li, P.R. Herman, in Proc. SPIE, vol. 4977 (2003), p. 400
68. T.V. Kononenko, S.V. Garnov, S.M. Pimenov, V.I. Konov, V. Romano, B. Borsos, H.P. Weber, Appl. Phys. A Mater. Sci. Process. **71**(6), 627 (2000)
69. T.V. Kononenko, V.V. Kononenko, V.I. Konov, S.M. Pimenov, S.V. Garnov, A.V. Tishchenko, A.M. Prokhorov, A.V. Khomich, Appl. Phys. A Mater. Sci. Process. **68**(1), 99 (1999)
70. J.R. Lankard, G. Wolbold, Appl. Phys. A Mater. Sci. Process. **54**(4), 355 (1992)
71. J. Ihlemann, K. Rubahn, Appl. Surf. Sci. **154**, 587 (2000)
72. D. Schäfer, J. Ihlemann, G. Marowsky, P. Herman, Appl. Phys. A Mater. Sci. Process. **72**(3), 377 (2001)

73. J. Ihlemann, K. Rubahn, R. Thielsch, in Proc. SPIE, vol. 4426 (2002), p. 437
74. K. Rubahn, J. Ihlemann, Appl. Surf. Sci. **127**, 881 (1998)
75. G.P. Behrmann, M.T. Duignan, Appl. Opt. **36**(20), 4666 (1997)
76. N.A. Vainos, S. Mailis, S. Pissadakis, L. Boutsikaris, P.J.M. Parmiter, P. Dainty, T.J. Hall, Appl. Opt. **35**(32), 6304 (1996)
77. X. Wang, J.R. Leger, R.H. Rediker, Appl. Opt. **36**(20), 4660 (1997)
78. F. Quentel, J. Fieret, A.S. Holmes, S. Paineau, in Proc. SPIE, vol. 4274 (2001), pp. 420–431
79. J. Ihlemann, D. Schäfer, Appl. Surf. Sci. **197**, 856 (2002)
80. J. Ihlemann, R. Weichenhain-Schriever, J. Laser Micro/Nanoeng. **4**, 100 (2009)
81. M. Schulz-Ruhtenberg, J. Ihlemann, J. Heber, Appl. Surf. Sci. **248**(1–4), 190 (2005)
82. H.M. Phillips, R.A. Sauerbrey, Opt. Eng. **32**(10), 2424 (1993)
83. P.E. Dyer, R.J. Farley, R. Giedl, D.M. Karnakis, Appl. Surf. Sci. **96**, 537 (1996)
84. J. Bekesi, J. Meinertz, J. Ihlemann, P. Simon, Appl. Phys. A Mater. Sci. Process. **93**(1), 27 (2008)
85. C.J. Newsome, M. O'Neill, R.J. Farley, G.P. Bryan-Brown, Appl. Phys. Lett. **72**(17), 2078 (1998)
86. M. Behdani, S.H. Keshmiri, S. Soria, M.A. Bader, J. Ihlemann, G. Marowsky, T. Rasing, Appl. Phys. Lett. **82**, 2553 (2003)
87. K.J. Ilcisin, R. Fedosejevs, Appl. Opt. **26**(2), 396 (1987)
88. H.M. Phillips, D.L. Callahan, R. Sauerbrey, G. Szabo, Z. Bor, Appl. Phys. Lett. **58**, 2761 (1991)
89. T. Lippert, T. Gerber, A. Wokaun, D.J. Funk, H. Fukumura, M. Goto, Appl. Phys. Lett. **75**, 1018 (1999)
90. K. Rubahn, J. Ihlemann, G. Jakopic, A.C. Simonsen, H.G. Rubahn, Appl. Phys. A Mater. Sci. Process. **79**(7), 1715 (2004)
91. S. Pissadakis, L. Reekie, M. Hempstead, M.N. Zervas, J.S. Wilkinson, Appl. Phys. A Mater. Sci. Process. **69**, 739 (1999)
92. M.A. Bader, C. Kappel, A. Selle, J. Ihlemann, M.L. Ng, P.R. Herman, Appl. Opt. **45**(25), 6586 (2006)
93. K. Naessens, P. Van Daele, R.G. Baets, in Proc. SPIE, vol. 4941 (2003), p. 133
94. K. Naessens, H. Ottevaere, R. Baets, P. Van Daele, H. Thienpont, Appl. Opt. **42**(31), 6349 (2003)
95. J.E.A. Pedder, A.S. Holmes, R. Allott, K. Boehlen, in Proc. SPIE, vol. 6462 (2007),
96. T. Lippert, A. Wokaun, Chimia **55**(10), 783 (2001)
97. T. Fricke-Begemann, J. Meinertz, J. Ihlemann, in EOS Topical Meeting on Micro-Optics, Diffractive Optics and Optical MEMS (Paris, 2006), p. 114
98. H.M. Presby, A.F. Benner, C.A. Edwards, Appl. Opt. **29**(18), 2692 (1990)
99. T. Fricke-Begemann, J. Li, J. Dou, J. Ihlemann, P. Herman, G. Marowsky, in Third International WLT-Conference Lasers in Manufacturing, LIM (2005), p. 733
100. J. Dou, J. Li, P.R. Herman, J.S. Aitchison, T. Fricke-Begemann, J. Ihlemann, G. Marowsky, Appl. Phys. A Mater. Sci. Process. **91**(4), 591 (2008)
101. M. Wehner, P. Jacobs, R. Poprawe, in Proc. SPIE, vol. 6459 (2007), p. 645908
102. W. Pfleging, R. Adamietz, H.J. Bruckner, M. Bruns, A. Welle, in Proc. SPIE, vol. 6459 (International Society for Optical Engineering, 2007), p. 645907
103. R. Böhme, B. Keiper, K. Zimmer, R. Ebert, H. Exner, in Proc. SPIE, vol. 5116 (2003), pp. 491–496
104. S. Nikumb, Q. Chen, C. Li, H. Reshef, H.Y. Zheng, H. Qiu, D. Low, Thin Solid Films **477** (1–2), 216 (2005)
105. D. Ashkenasi, M. Schwagmeier, in Proc. SPIE, vol. 6458 (2007), p. 64580F
106. P.R. Herman, A. Yick, J. Li, N. Munce, L. Lilge, E. Jervis, S. Krylov, in CLEO Tech. Digest CLF5 (2003), p. 3
107. P.E. Dyer, S.M. Maswadi, C.D. Walton, M. Ersoz, P.D.I. Fletcher, V.N. Paunov, Appl. Phys. A Mater. Sci. Process. **77**(3), 391 (2003)
108. S.J. Qin, W.J. Li, Appl. Phys. A Mater. Sci. Process. **74**(6), 773 (2002)